NASA TM X-144

TECHNICAL MEMORANDUM

X-144

LOW-SPEED MEASUREMENTS OF OSCILLATORY LATERAL STABILITY DERIVATIVES OF A 1/7-SCALE MODEL OF THE NORTH AMERICAN X-15 AIRPLANE

By John W. Paulson and James L. Hassell, Jr.

Langley Research Center
Langley Field, Va.

NATIONAL AERONAUTICS AND SPACE ADMINISTRATION

WASHINGTON

November 1959
Declassified May 29, 1961

NATIONAL AERONAUTICS AND SPACE ADMINISTRATION

TECHNICAL MEMORANDUM X-144

LOW-SPEED MEASUREMENTS OF OSCILLATORY LATERAL STABILITY DERIVATIVES OF A 1/7-SCALE MODEL OF THE NORTH AMERICAN X-15 AIRPLANE

By John W. Paulson and James L. Hassell, Jr.

SUMMARY

An investigation to determine the low-speed rolling, yawing, and sideslipping derivatives of a 1/7-scale model which was used to represent the original configuration and a modified configuration of the North American X-15 airplane has been conducted in the Langley free-flight tunnel. The original model was modified to approximately represent the final airplane configuration by reducing the size of the fuselage side fairings and changing the vertical-tail arrangement. The effects of various tail arrangements were determined for both configurations and the effect of small forebody strakes was determined for the modified configuration only.

INTRODUCTION

An investigation has been made to determine the low-speed rolling, yawing, and sideslipping derivatives of a 1/7-scale model which was used to represent the original configuration and a modified configuration of the North American X-15 airplane. The airplane has a large fuselage, a short-span low-aspect-ratio wing, and a large all-movable horizontal tail which is used for roll control as well as pitch control.

The investigation included rolling and yawing oscillation tests of the original configuration (fuselage fairings starting at the nose and a vertical tail having most of its area above the fuselage) and rolling, yawing, and sideslipping tests of the modified configuration (fuselage fairings starting at about midcanopy and a vertical tail having nearly equal areas above and below the fuselage) for various tail arrangements. In addition the modified model was tested with longitudinal nose strakes.

The investigation was made over an angle-of-attack range from 0° to 36° for the original configuration and over an angle-of-attack range from 0° to 60° for the modified model. A range of reduced-frequency values from 0.020 to 0.170 was studied.

DEFINITION OF TERMS AND SYMBOLS

The longitudinal data are referred to the stability axes. All lateral stability parameters and coefficients are referred to the body system of axes originating at a center-of-gravity position of 25 percent of the mean aerodynamic chord for the original configuration and 16 percent of the mean aerodynamic chord for the modified configuration. (See fig. 1.) The term "in-phase derivative" used herein refers to any one of the stability derivatives that are based on the forces or moments in phase with the angle of roll, yaw, or sideslip produced in the oscillatory tests. The term "out-of-phase derivative" refers to any one of the stability derivatives that are based on the forces or moments 90° out of phase with the angle of roll, yaw, or sideslip. The derivatives measured in the investigation are summarized in table I. All measurements are reduced to standard coefficient form and are presented in terms of the following symbols:

X, Y, Z	body reference axes unless otherwise noted
S	wing area, sq ft
b	wing span, ft
$\bar{c}$	mean aerodynamic chord, ft
V	free-stream velocity, ft/sec
q	free-stream dynamic pressure, lb/sq ft
ω	angular velocity, $2\pi f$, radians/sec
f	frequency of oscillation, cps
k	reduced-frequency parameter, $\omega b/2V$
α	angle of attack, deg
β	angle of sideslip, deg or radians
r	yawing velocity, radians/sec

p rolling velocity, radians/sec

$\dot{\beta} = \frac{d\beta}{dt}$

$\dot{r} = \frac{dr}{dt}$

$\dot{p} = \frac{dp}{dt}$

F_X axial force, lb

F_N normal force, lb

F_L lift, lb

F'_D drag, lb

F_Y side force, lb

M_Y pitching moment, ft-lb

M_X rolling moment, ft-lb

M_Z yawing moment, ft-lb

C_m pitching-moment coefficient, $\frac{M_Y}{qS\bar{c}}$

C_l rolling-moment coefficient, $\frac{M_X}{qSb}$

C_n yawing-moment coefficient, $\frac{M_Z}{qSb}$

C_L lift coefficient, $\frac{F_L}{qS}$

C'_D drag coefficient, $\frac{F'_D}{qS}$

C_Y side-force coefficient, $\frac{F_Y}{qS}$

t time, sec

ϕ angle of roll, radians

ψ angle of yaw, radians

$$C_{l_\beta} = \frac{\partial C_l}{\partial \beta}, \text{ per radian}$$

$$C_{n_\beta} = \frac{\partial C_n}{\partial \beta}, \text{ per radian}$$

$$C_{Y_\beta} = \frac{\partial C_Y}{\partial \beta}, \text{ per radian}$$

$$C_{l_r} = \frac{\partial C_l}{\partial \frac{rb}{2V}} \qquad C_{n_r} = \frac{\partial C_n}{\partial \frac{rb}{2V}} \qquad C_{Y_r} = \frac{\partial C_Y}{\partial \frac{rb}{2V}}$$

$$C_{l_p} = \frac{\partial C_l}{\partial \frac{pb}{2V}} \qquad C_{n_p} = \frac{\partial C_n}{\partial \frac{pb}{2V}} \qquad C_{Y_p} = \frac{\partial C_Y}{\partial \frac{pb}{2V}}$$

$$C_{l_{\dot\beta}} = \frac{\partial C_l}{\partial \frac{\dot\beta b}{2V}} \qquad C_{n_{\dot\beta}} = \frac{\partial C_n}{\partial \frac{\dot\beta b}{2V}} \qquad C_{Y_{\dot\beta}} = \frac{\partial C_Y}{\partial \frac{\dot\beta b}{2V}}$$

$$C_{l_{\dot r}} = \frac{\partial C_l}{\partial \frac{\dot r b^2}{4V^2}} \qquad C_{n_{\dot r}} = \frac{\partial C_n}{\partial \frac{\dot r b^2}{4V^2}} \qquad C_{Y_{\dot r}} = \frac{\partial C_Y}{\partial \frac{\dot r b^2}{4V^2}}$$

$$C_{l_{\dot p}} = \frac{\partial C_l}{\partial \frac{\dot p b^2}{4V^2}} \qquad C_{n_{\dot p}} = \frac{\partial C_n}{\partial \frac{\dot p b^2}{4V^2}} \qquad C_{Y_{\dot p}} = \frac{\partial C_Y}{\partial \frac{\dot p b^2}{4V^2}}$$

APPARATUS AND MODELS

The static tests and the rotary and linear oscillation tests were conducted in the Langley free-flight tunnel. Detailed descriptions of the oscillation apparatus and the methods used in deriving the data are given in reference 1. The models were sting mounted and the forces and moments were measured about the body axes by means of a three-component internal strain-gage balance.

The 1/7-scale model (flaps-up configuration) of reference 2 was used as the original configuration. This model was modified to approximately represent the final configuration by reducing the size of the fuselage fairings and changing the vertical tail. (See fig. 2.) In addition to these modifications the final configuration should have had an increase in fuselage diameter (fig. 3(a)), but the test model did not duplicate this feature. Strakes were also added to the modified model for a part of the investigation. (See fig. 3(b).)

TESTS

The static longitudinal characteristics of the original configuration with horizontal tail on and off were measured over a range of angles of attack from 0° to 40° while the static lateral characteristics with upper vertical tail on and off were measured over a range of angles of attack from 0° to 36°. The static longitudinal and lateral characteristics of the modified configuration with strakes off and on were measured over a range of angles of attack from 0° to 60°. The lateral stability characteristics were determined for the model with all tails on, with lower rudder off, and with all vertical tails off.

The rolling oscillation tests for the original configuration were made over a range of angles of attack from 0° to 36° with all tails on, upper vertical tail off, and all tails off, while the yawing oscillation tests were made only with all tails on and all tails off. These tests were made for a range of values of the reduced-frequency parameter $\omega b/2V$ from 0.020 to 0.170. The rolling, yawing, and sideslipping oscillation tests for the modified configuration with strakes off and on were made over a range of angles of attack from 0° to 60° with all tails on, lower rudder off, and all vertical tails off, for values of the reduced-frequency parameter of 0.070, 0.105, and 0.140. In the tail-off tests of the original configuration only the movable portions of the tail surfaces (all of horizontal and 87.5 percent of upper vertical) were removed, whereas in the tail-off tests of the modified configuration all of the vertical surfaces including stubs were removed.

The tests of the original configuration were made at a dynamic pressure of 5.1 pounds per square foot which corresponds to a velocity of about 67 feet per second and a Reynolds number of 630,000 based on the mean aerodynamic chord of 1.47 feet, while the tests for the modified configuration were made at a dynamic pressure of 5.8 pounds per square foot which corresponds to a Reynolds number of 675,000.

RESULTS

The results of this investigation are presented herein without discussion. The static longitudinal and lateral stability characteristics of the original and modified configurations are presented in figures 4 and 5, respectively. These data for the original configuration are from reference 2 and are presented here to afford a more convenient correlation with the data on the oscillatory derivatives. The lateral derivatives were obtained by measuring at low angles of sideslip the slope of the C_Y, C_n, and C_l curves plotted against angle of sideslip. Since these curves were generally nonlinear (particularly the strakes-off data) the derivatives should be used only to give an indication of the trends.

The data obtained from the rolling and yawing oscillation tests are presented in figures 6 to 9 and figures 10 to 13, respectively, for both configurations. The data obtained from the sideslipping oscillation tests are presented in figures 14 and 15 for the modified configuration. The data presented for the original configuration were obtained by cross plotting for the values of the reduced-frequency parameter at which the modified model was run.

Langley Research Center,
National Aeronautics and Space Administration,
Langley Field, Va., August 5, 1959.

REFERENCES

1. Hewes, Donald E.: Low-Subsonic Measurements of the Static and Oscillatory Lateral Stability Derivatives of a Sweptback-Wing Airplane Configuration at Angles of Attack From -10° to 90°. NASA MEMO 5-20-59L, 1959.

2. Boisseau, Peter C.: Investigation of the Low-Speed Stability and Control Characteristics of a 1/7-Scale Model of the North American X-15 Airplane. NACA RM L57D09, 1957.

TABLE I

DERIVATIVES MEASURED IN OSCILLATORY TESTS

	Rolling	Yawing	Sideslipping
In-phase derivatives	$C_{l_\beta} \sin \alpha - k^2 C_{l_{\dot{p}}}$	$C_{l_\beta} \cos \alpha + k^2 C_{l_{\dot{r}}}$	C_{l_β}
	$C_{n_\beta} \sin \alpha - k^2 C_{n_{\dot{p}}}$	$C_{n_\beta} \cos \alpha + k^2 C_{n_{\dot{r}}}$	C_{n_β}
	$C_{Y_\beta} \sin \alpha - k^2 C_{Y_{\dot{p}}}$	$C_{Y_\beta} \cos \alpha + k^2 C_{Y_{\dot{r}}}$	C_{Y_β}
Out-of-phase derivatives	$C_{l_p} + C_{l_{\dot{\beta}}} \sin \alpha$	$C_{l_r} - C_{l_{\dot{\beta}}} \cos \alpha$	$C_{l_{\dot{\beta}}}$
	$C_{n_p} + C_{n_{\dot{\beta}}} \sin \alpha$	$C_{n_r} - C_{n_{\dot{\beta}}} \cos \alpha$	$C_{n_{\dot{\beta}}}$
	$C_{Y_p} + C_{Y_{\dot{\beta}}} \sin \alpha$	$C_{Y_r} - C_{Y_{\dot{\beta}}} \cos \alpha$	$C_{Y_{\dot{\beta}}}$

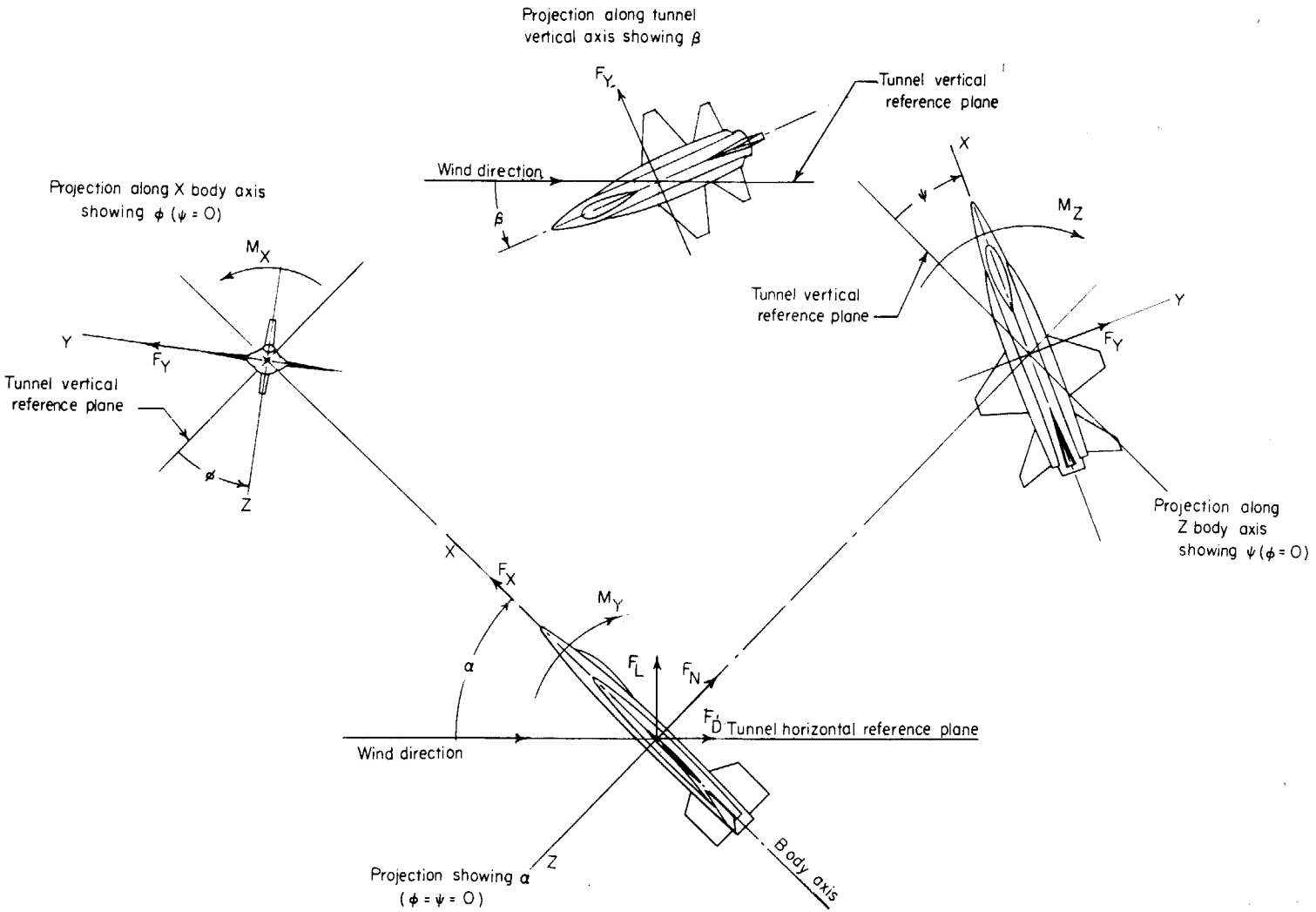

Figure 1.- System of axes used in the investigation. Arrows indicate positive directions of moments, forces, and angles.

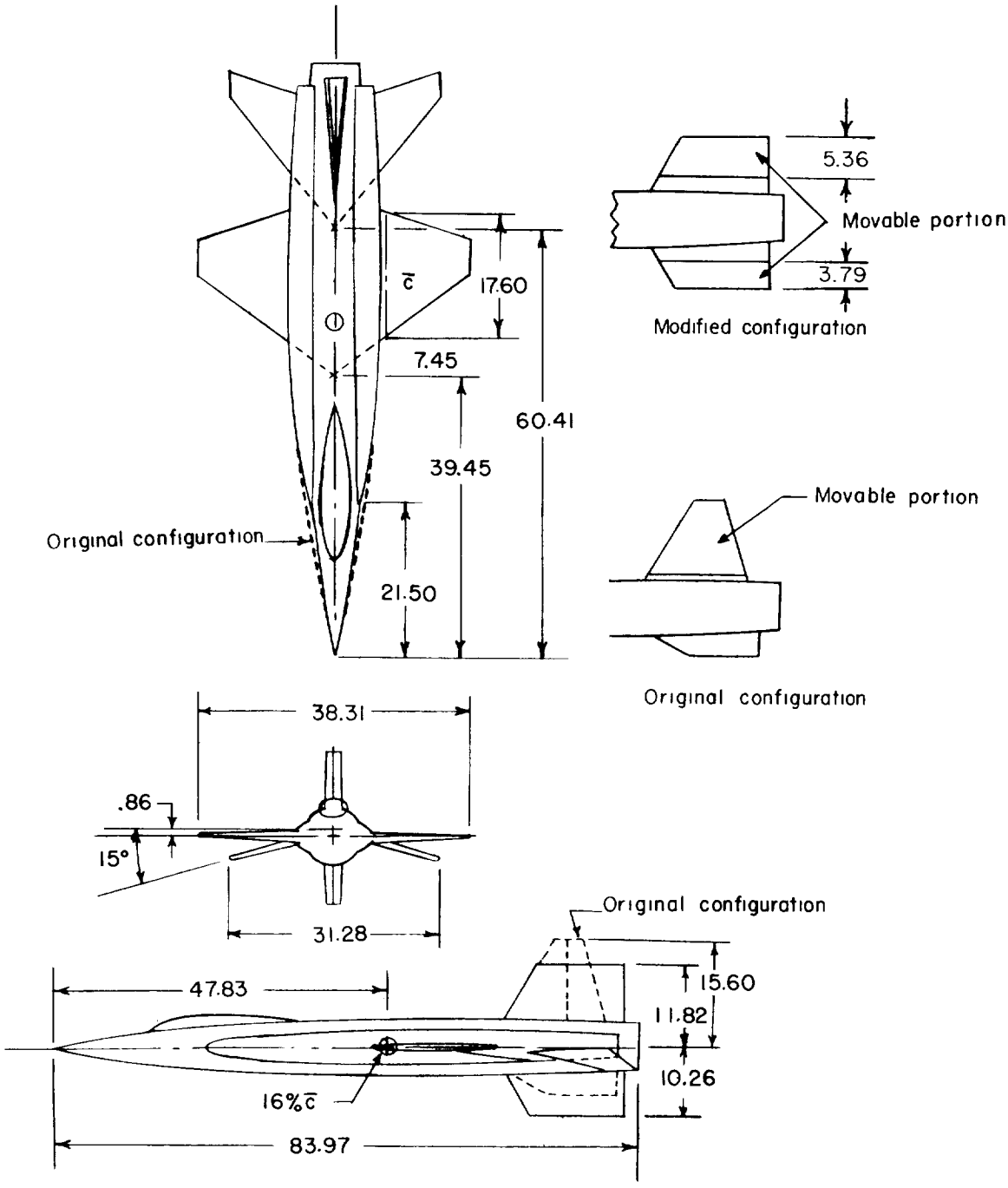

Figure 2.- Three-view drawing of models used in investigation. All dimensions are in inches.

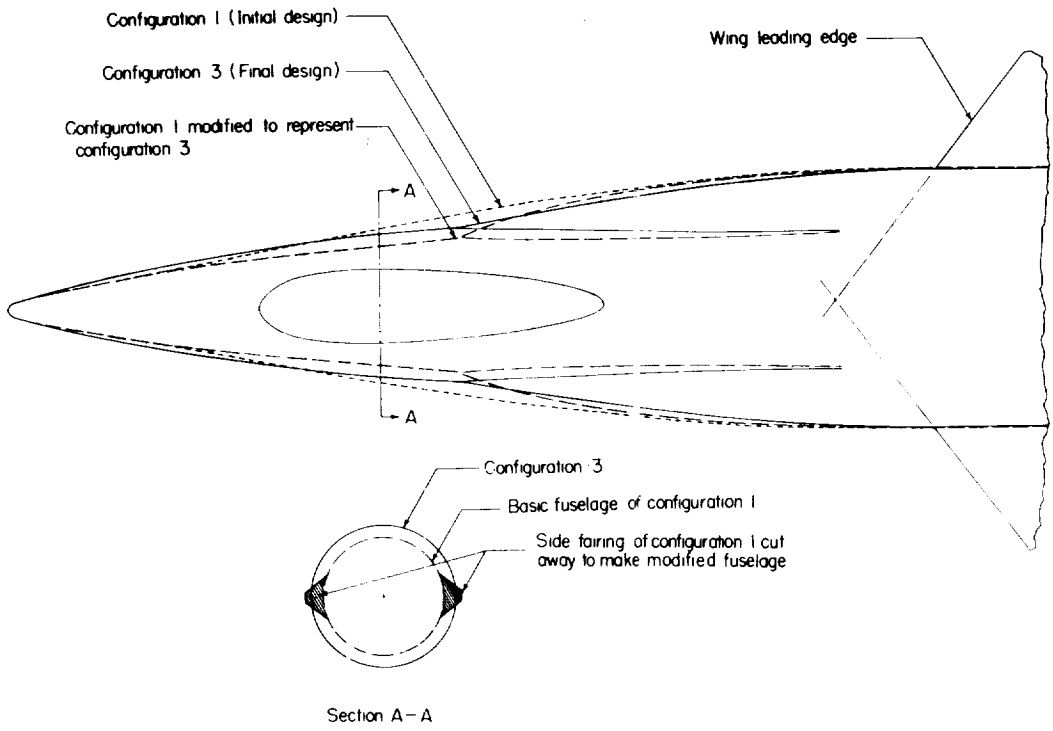

(a) Forebody modification.

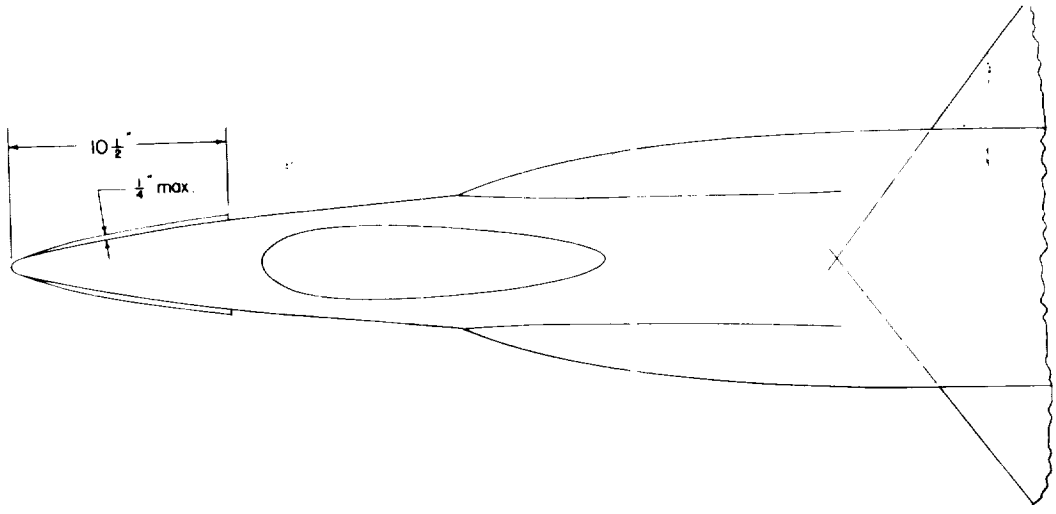

(b) Strake installation on modified model.

Figure 3.- Details of fuselage side-fairing alteration and strake installation on modified model.

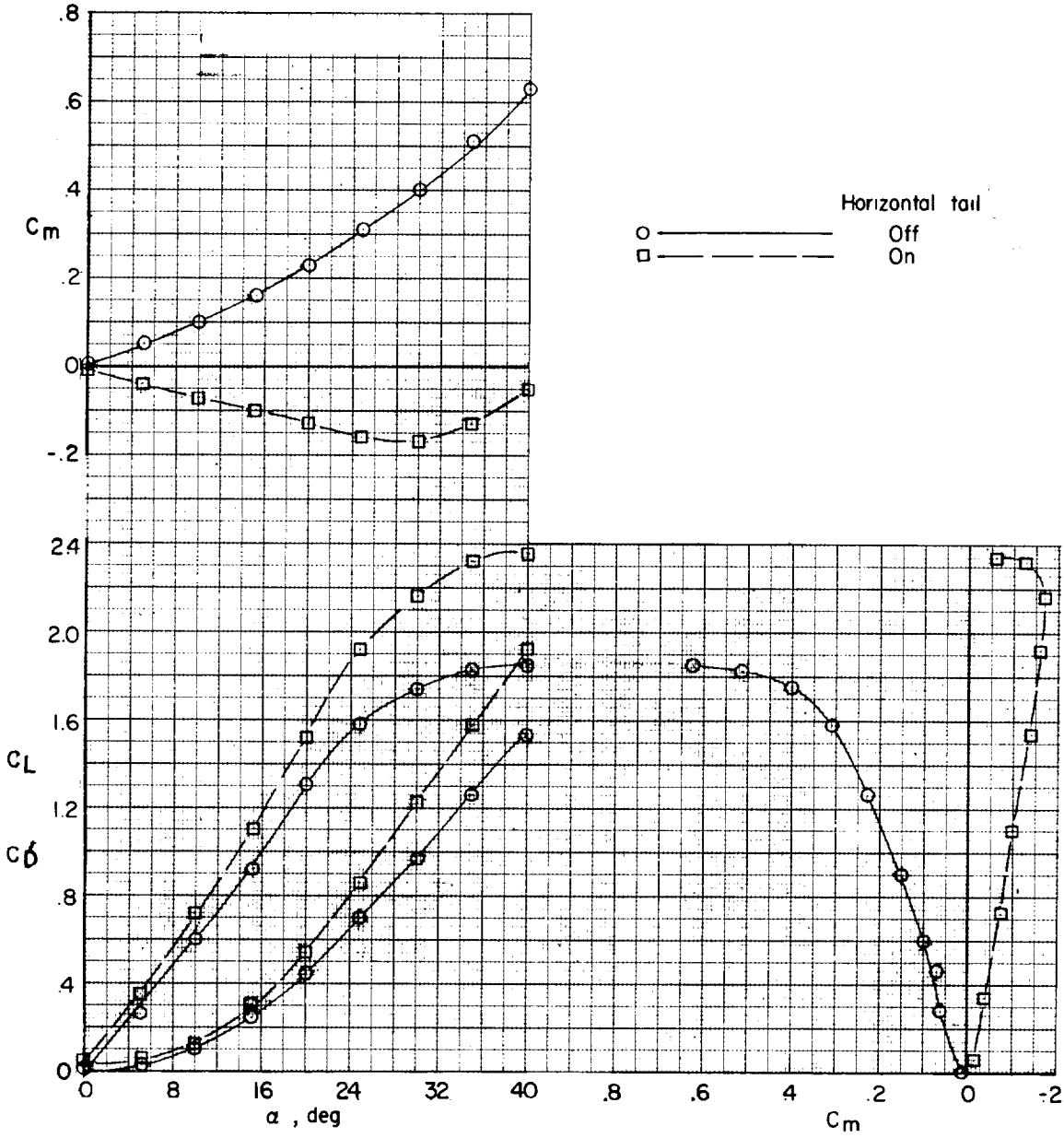

(a) Original configuration; center of gravity at $0.25\bar{c}$.

Figure 4.- Static longitudinal characteristics.

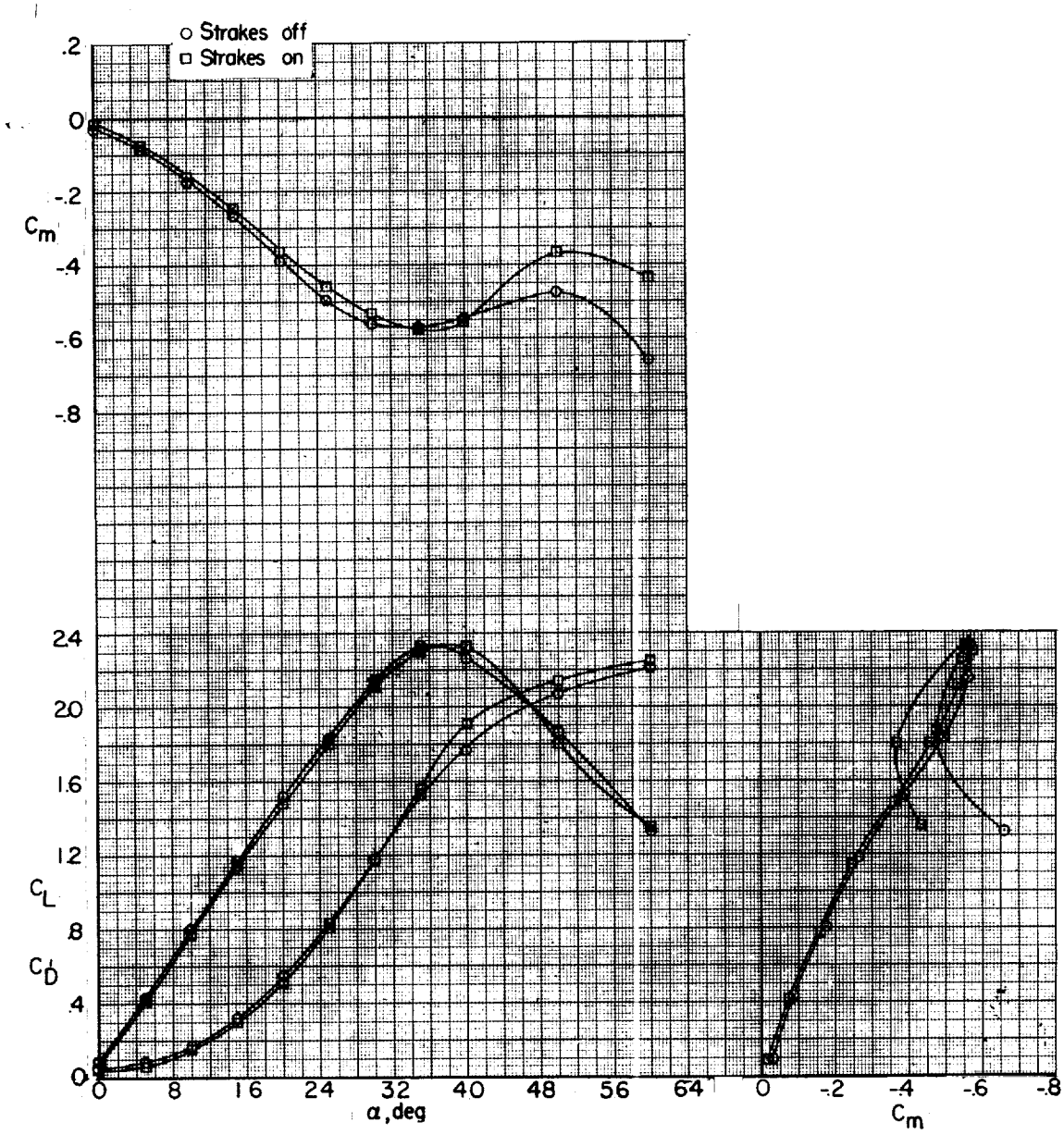

(b) Modified configuration; center of gravity at $0.16\bar{c}$.

Figure 4.- Concluded.

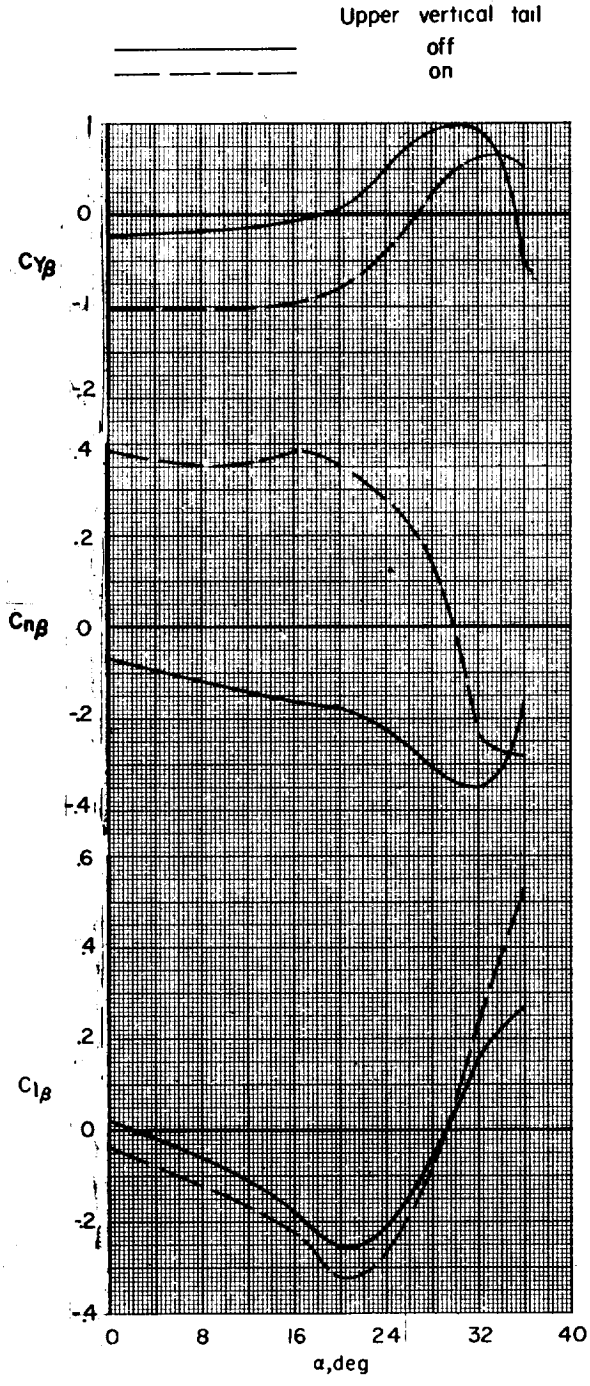

(a) Original configuration.

Figure 5.- Static lateral stability characteristics.

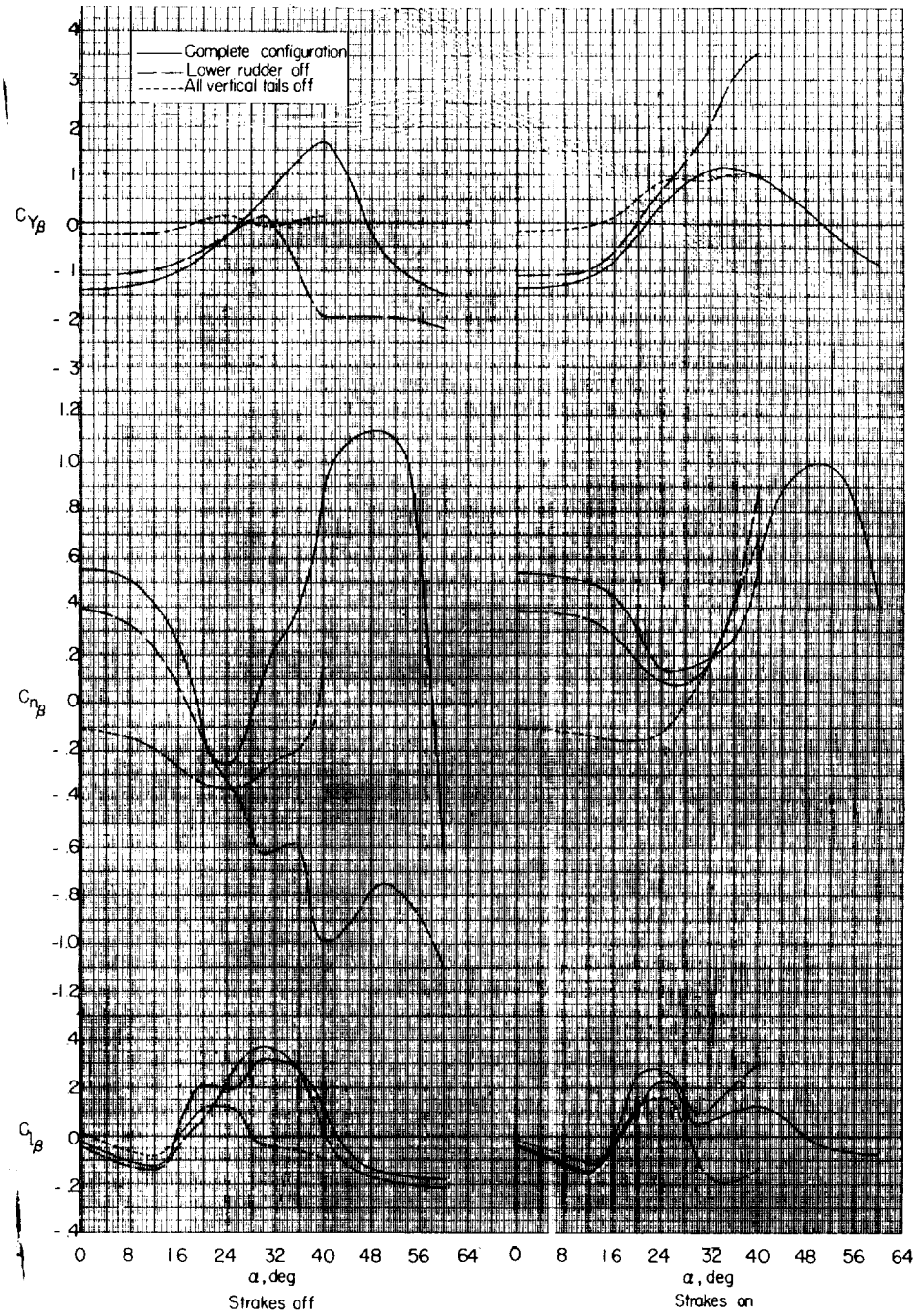

(b) Modified configuration.

Figure 5.- Concluded.

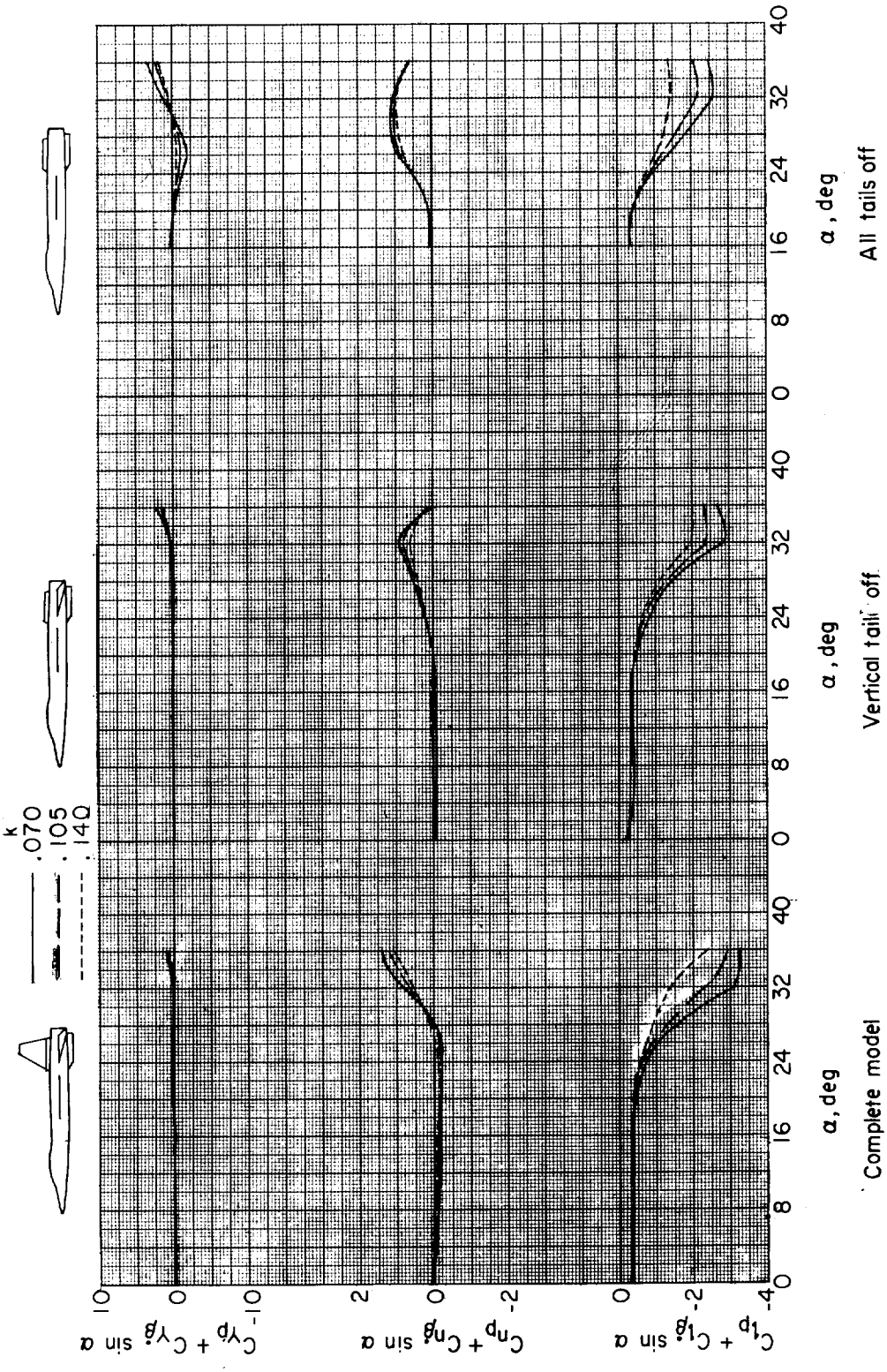

Figure 6.- Out-of-phase rolling derivatives of original configuration.

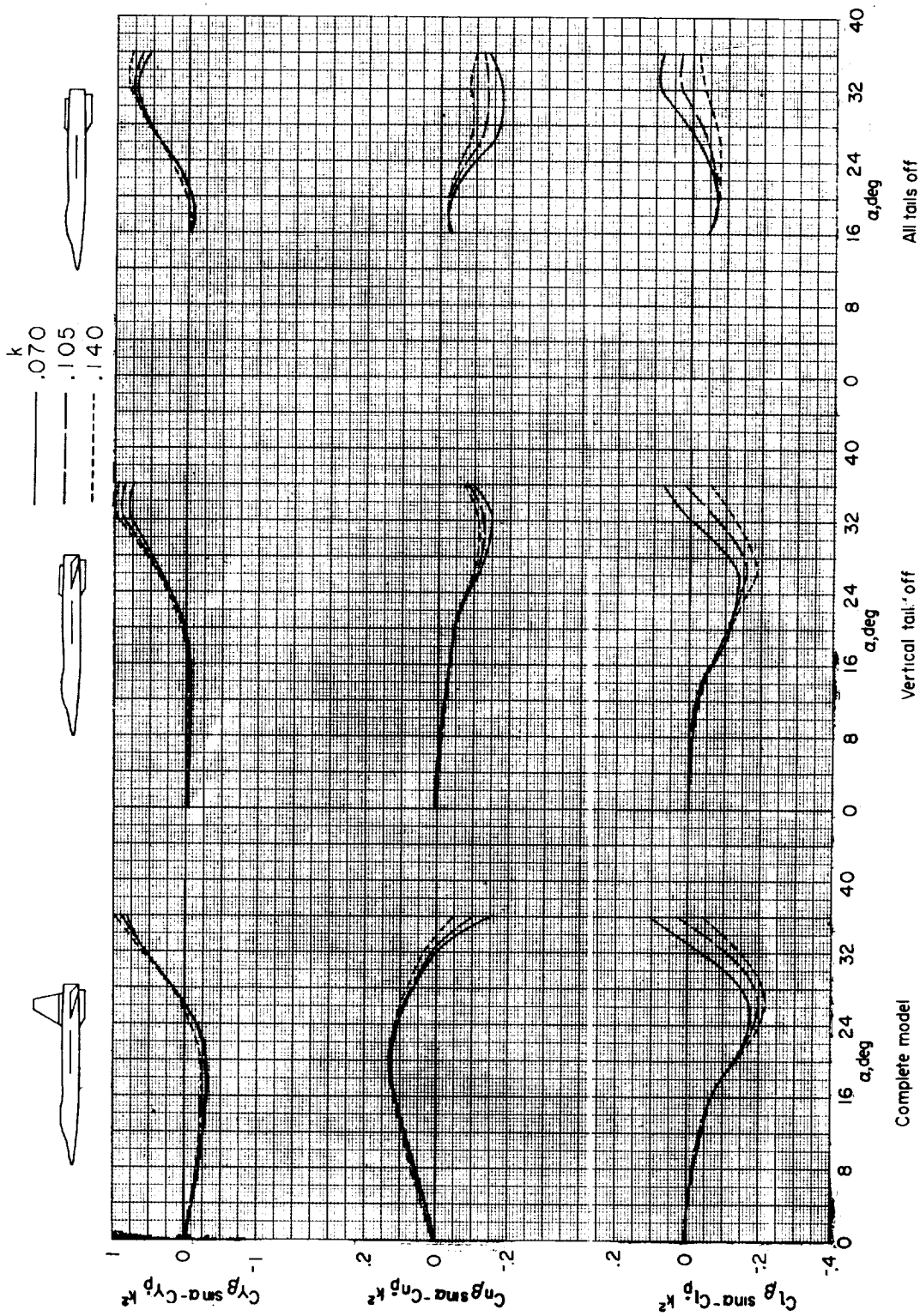

Figure 7.- In-phase rolling derivatives of original configuration.

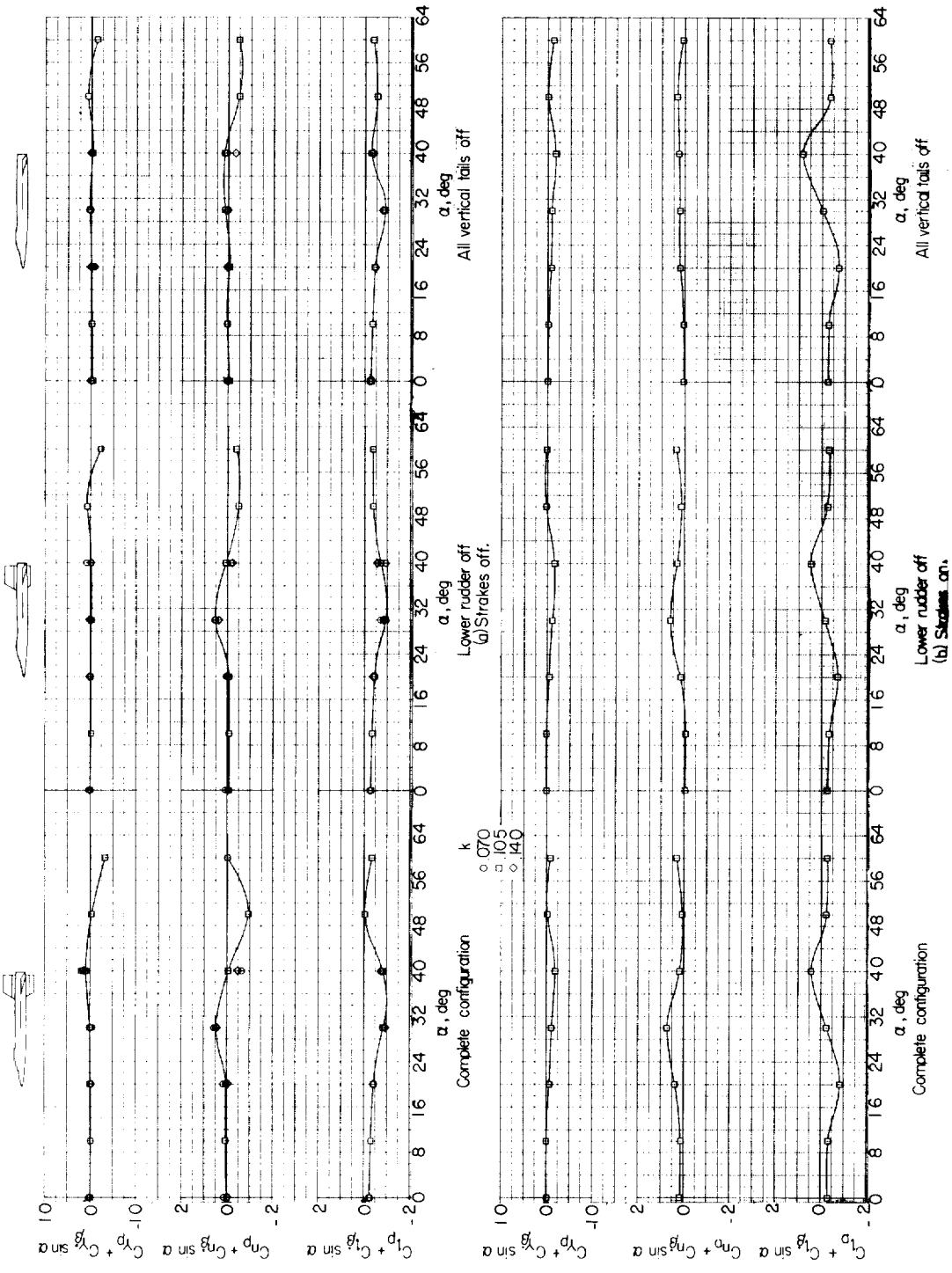

Figure 8.- Out-of-phase rolling derivatives of modified configuration.

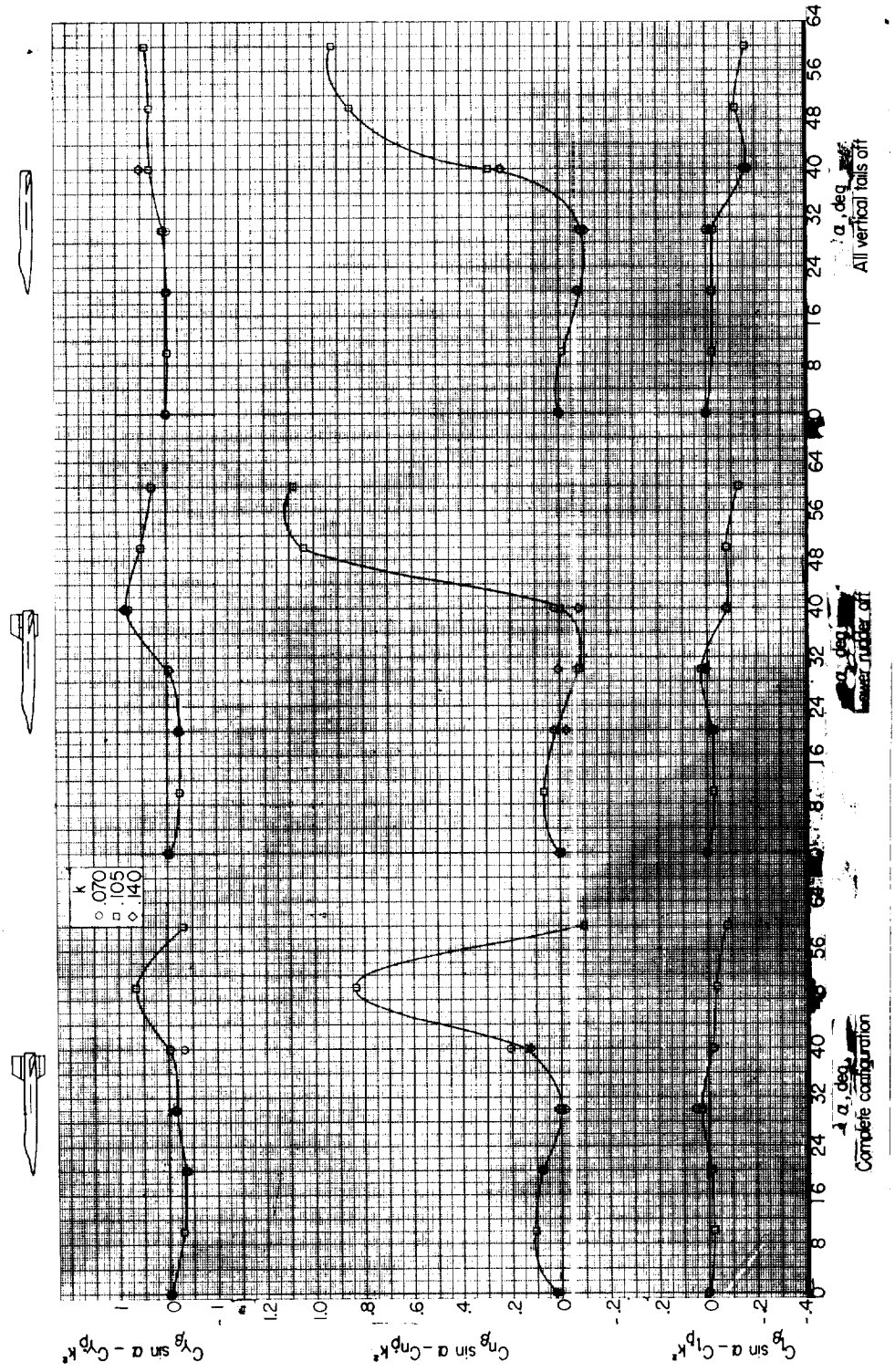

(a) Strakes off.

Figure 9.- In-phase rolling derivatives of modified configuration.

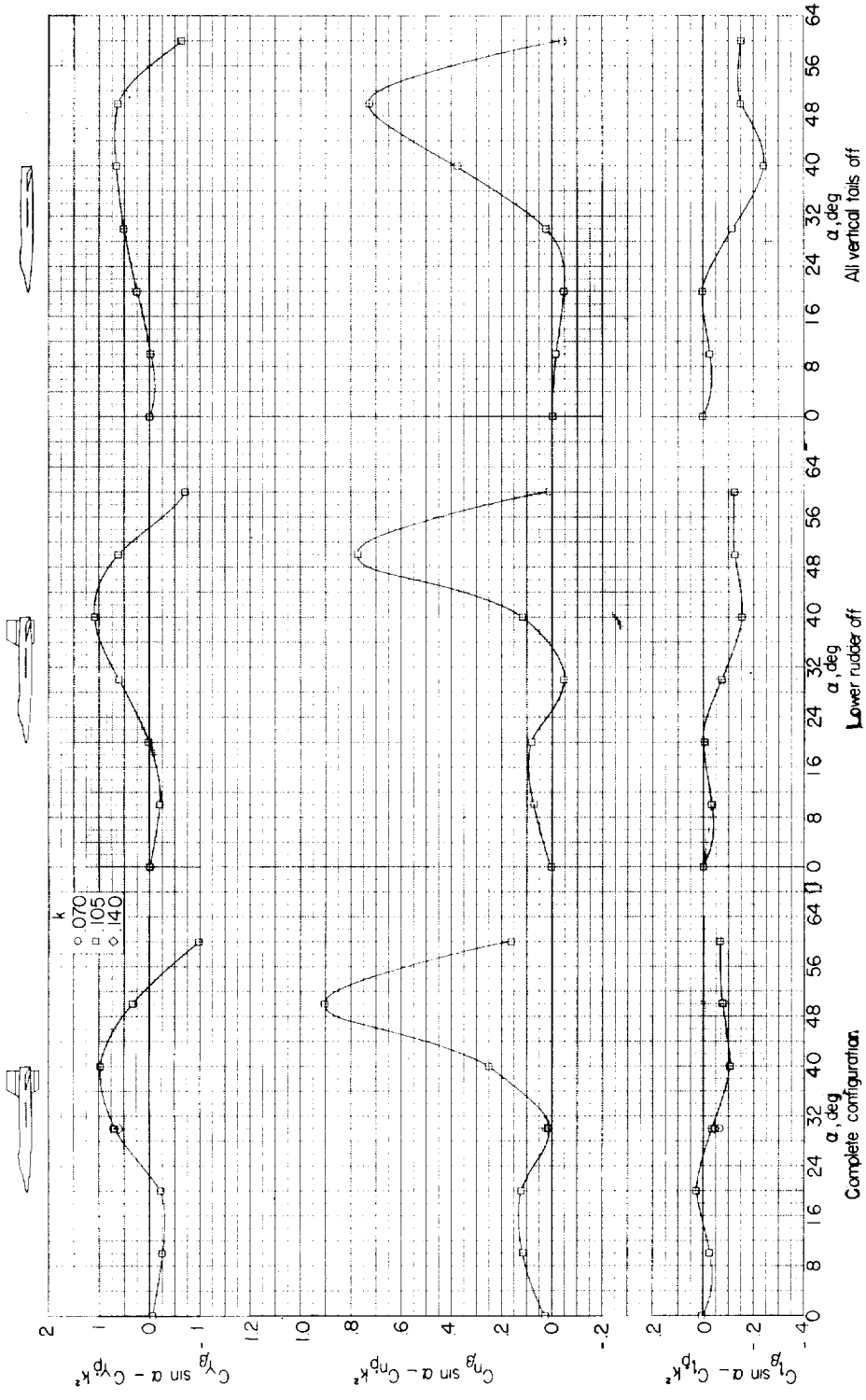

(b) Strakes on.

Figure 9.- Concluded.

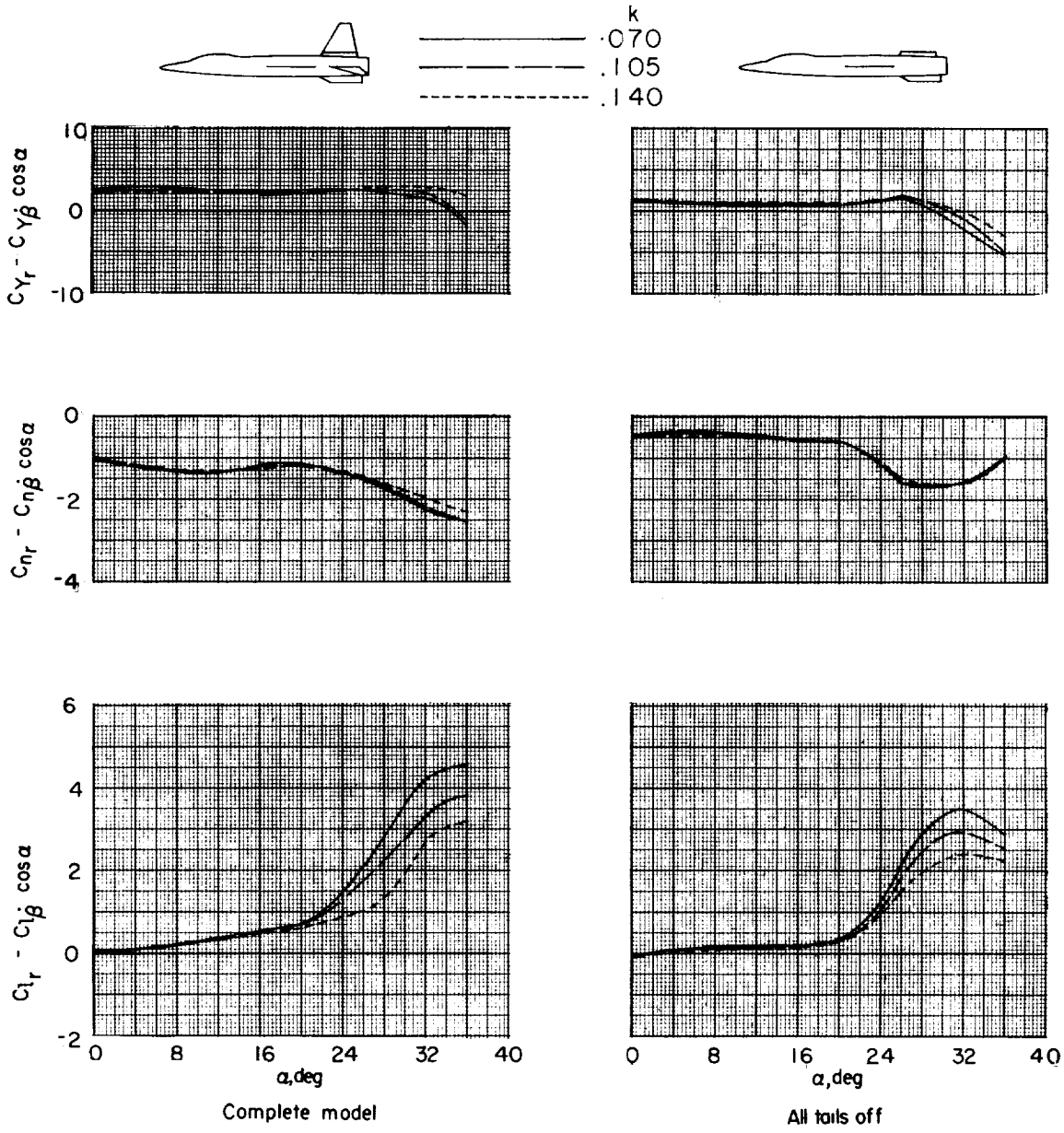

Figure 10.- Out-of-phase yawing derivatives of original configuration.

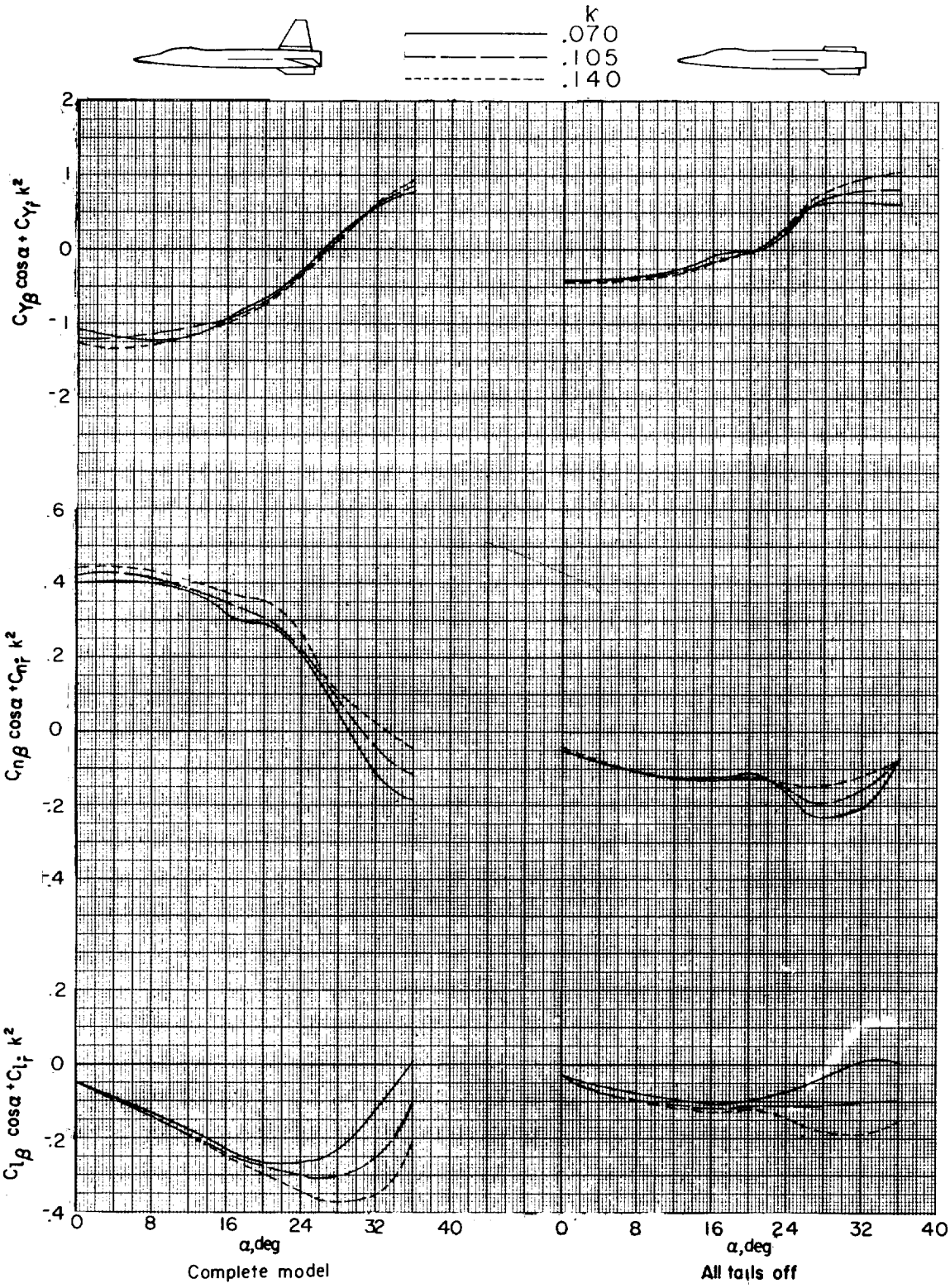

Figure 11.- In-phase yawing derivatives of original configuration.

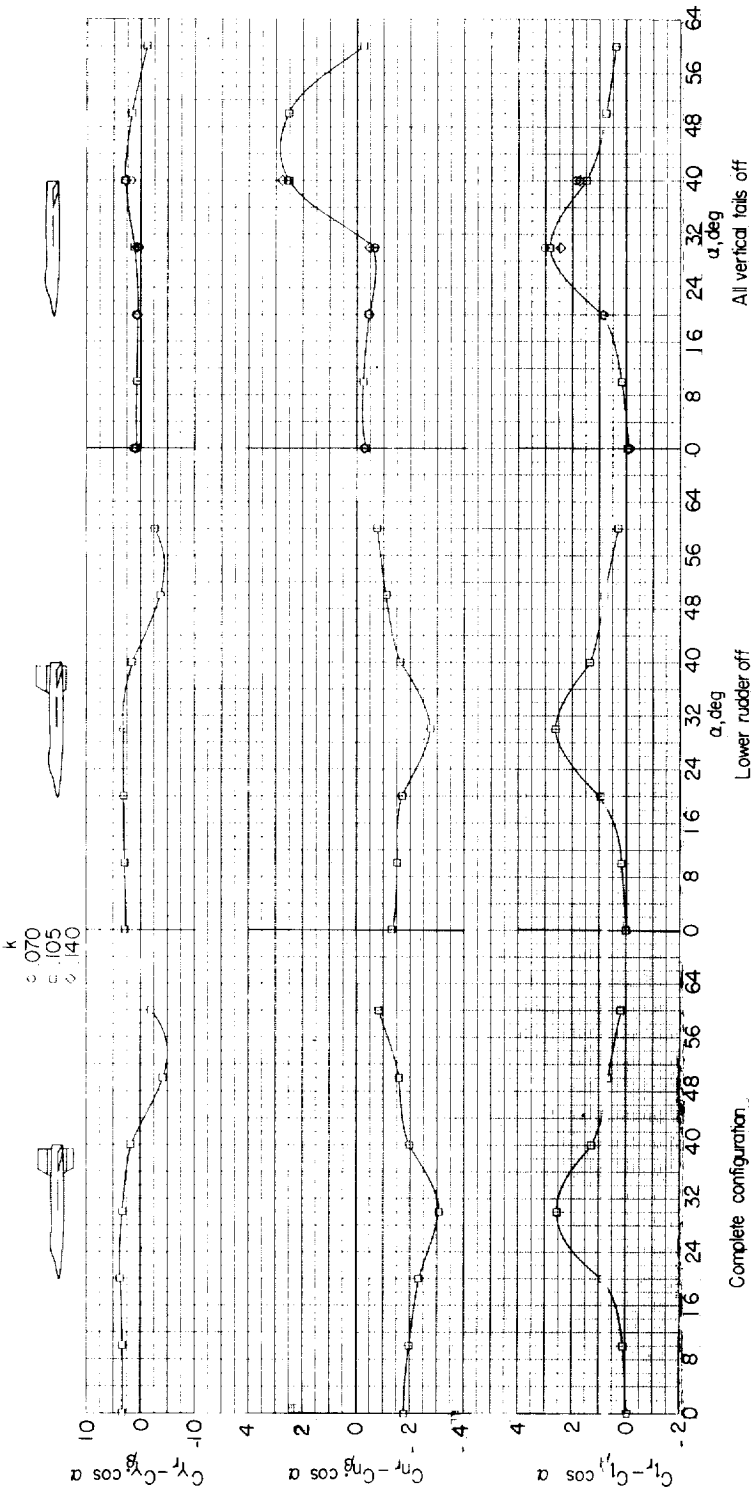

(a) Strakes off.

Figure 12.- Out-of-phase yawing derivatives of modified configuration.

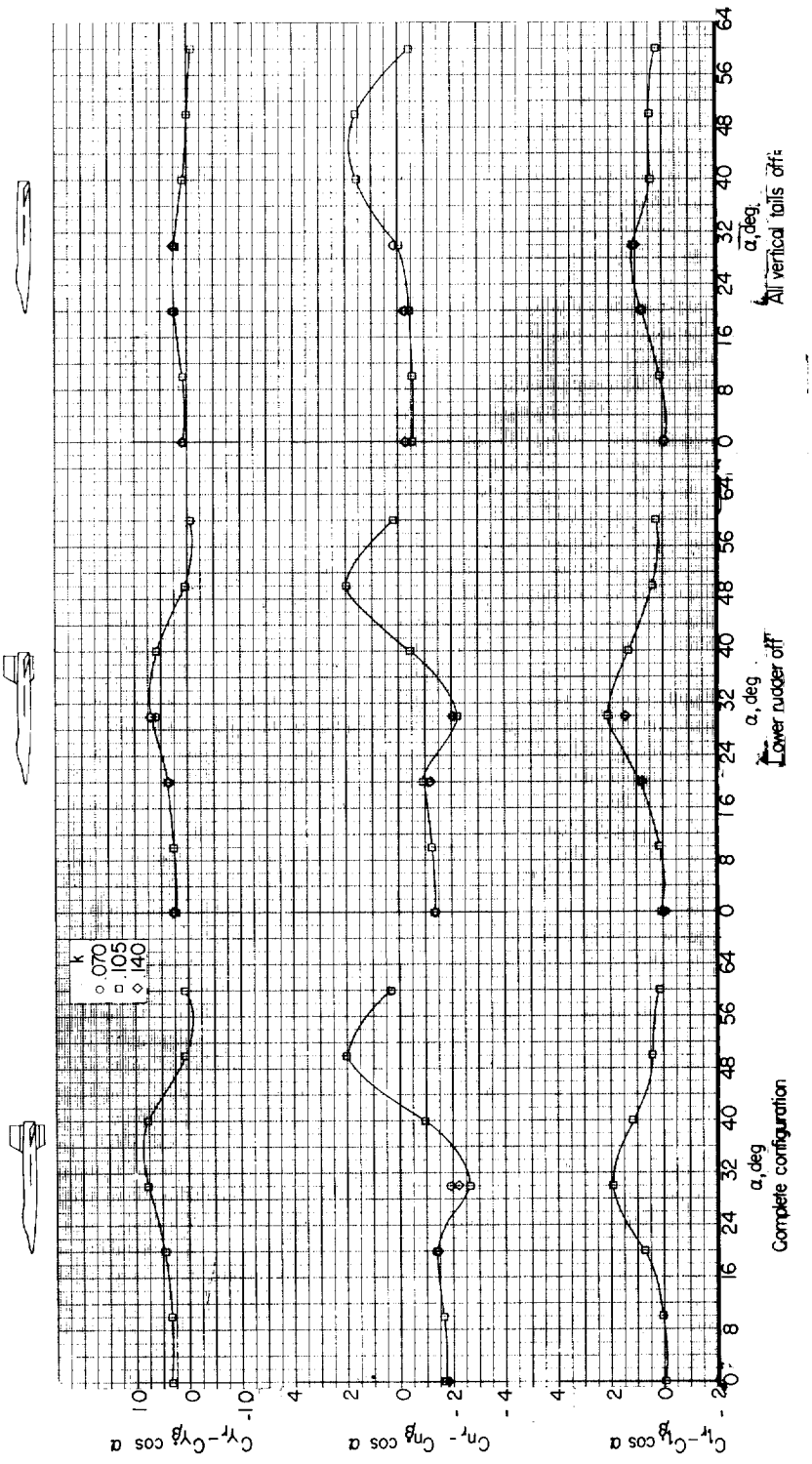

(b) Strakes on.

Figure 12.- Concluded.

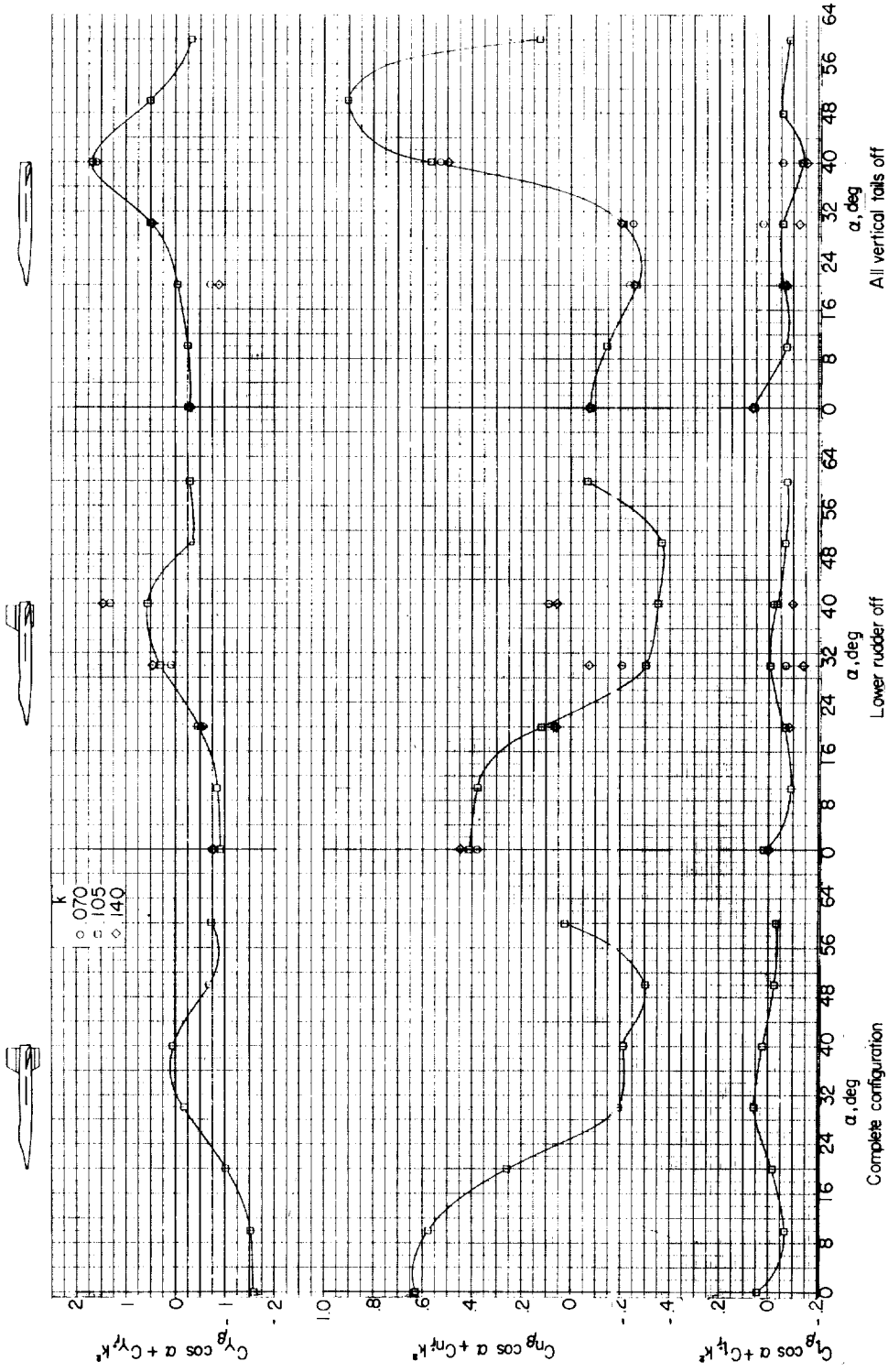

(a) Strakes off.

Figure 13.- In-phase yawing derivatives of modified configuration.

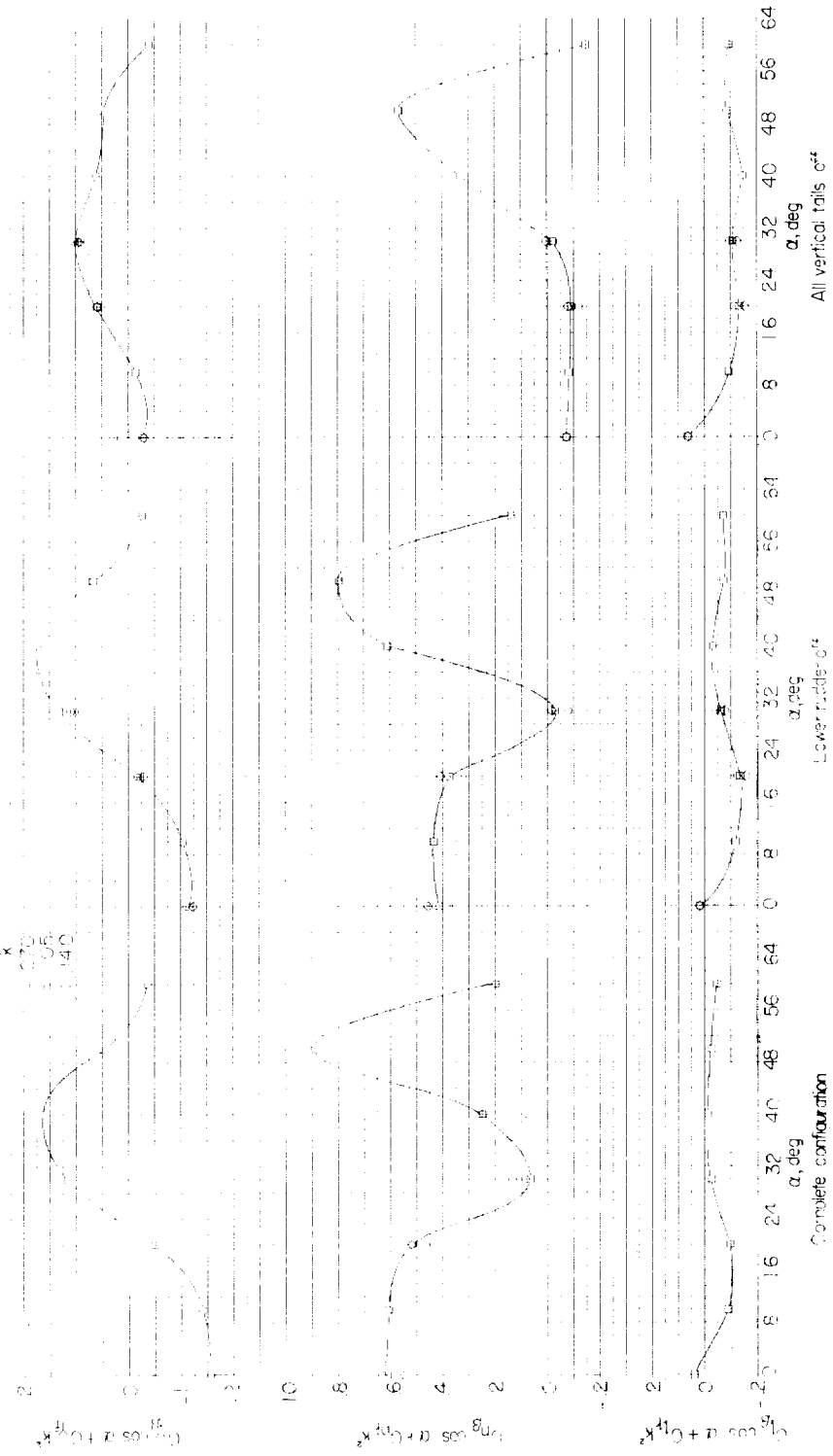

(b) Stresses on.

Figure 13. - Concluded.

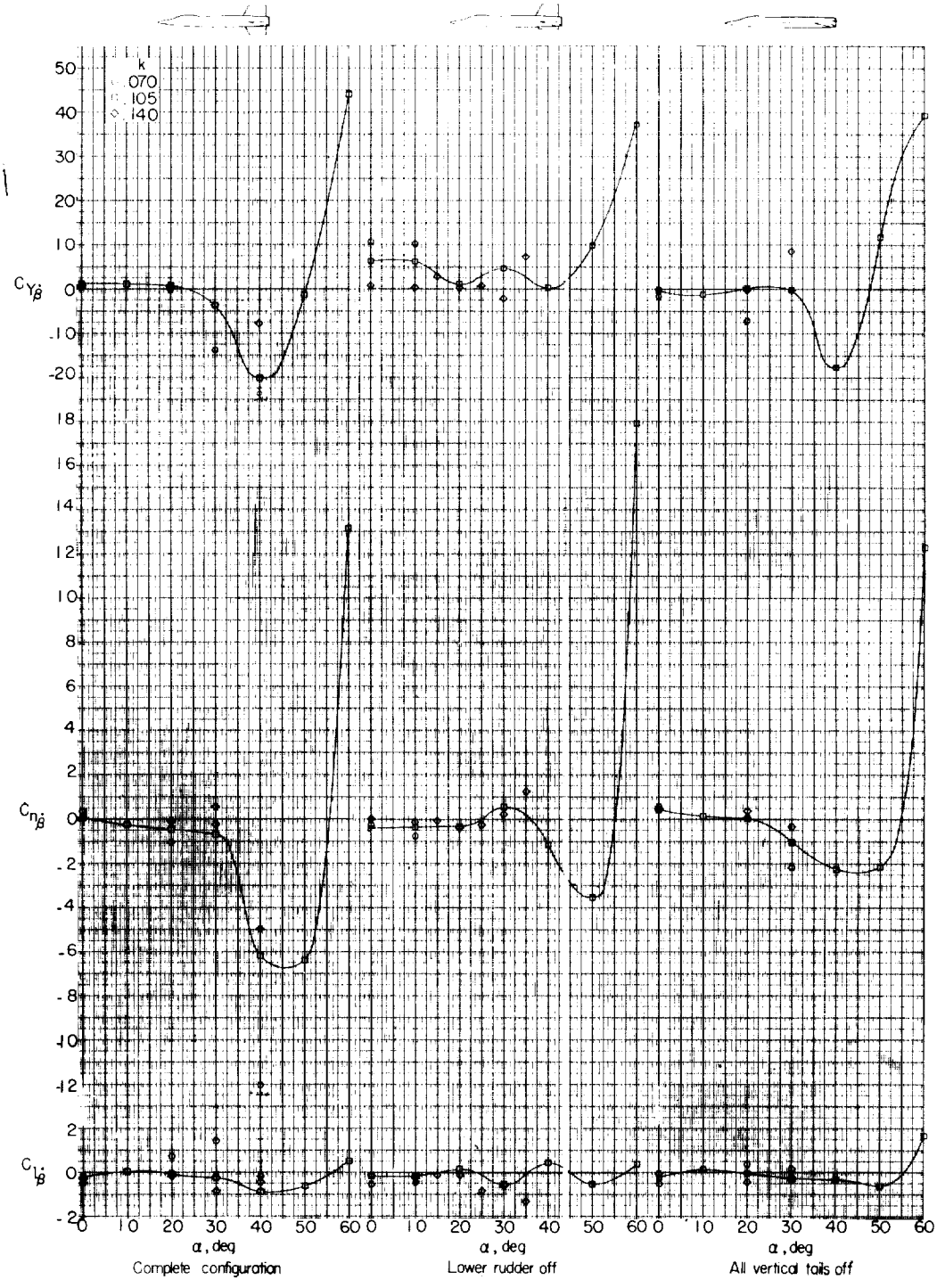

Figure 14.- Out-of-phase sideslipping derivatives of modified configuration; strakes off.

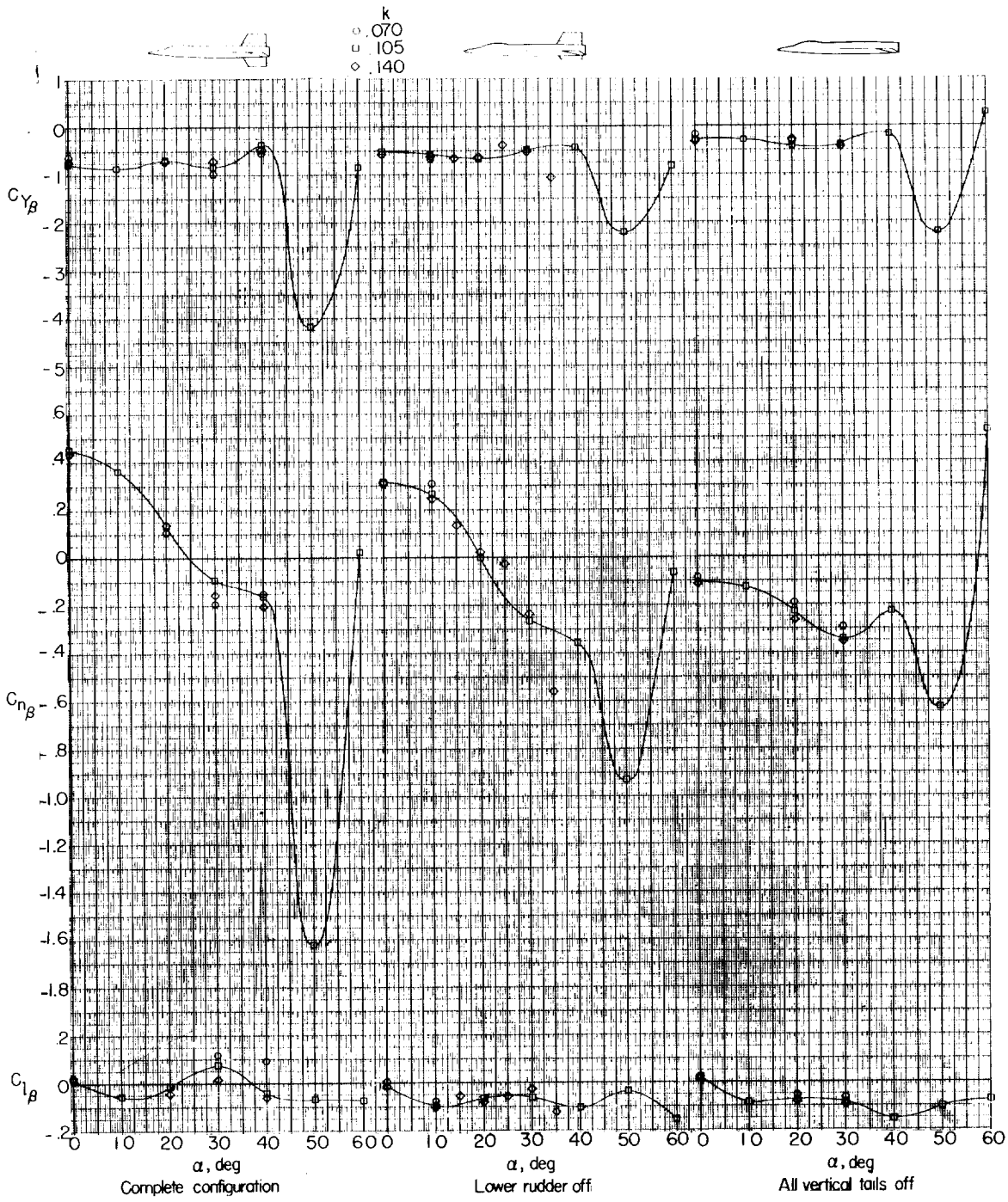

Figure 15.- In-phase sideslipping derivatives of modified configuration; strakes off.